

DOI:10.13476/j.cnki.nsbdqk.2022.0034

宋铁燕,陈莹,雷享勇,等.山美水库流域极端降水时空变化及非平稳性特征[J].南水北调与水利科技(中英文),2022,20(2):327-337,364. SONG T Y, CHEN Y, LEI X Y, et al. Temporal and spatial variation and non-stationary characteristics of extreme precipitation in the Shanmei reservoir basin[J]. South-to-North Water Transfers and Water Science & Technology, 2022, 20(2):327-337, 364. (in Chinese)

# 山美水库流域极端降水时空变化及非平稳性特征

宋铁燕<sup>1</sup>,陈莹<sup>1,2,3</sup>,雷享勇<sup>1</sup>,陈兴伟<sup>1,2,3</sup>,高路<sup>1,2,3</sup>,刘梅冰<sup>1,2,3</sup>,邓海军<sup>1,2,3</sup>

(1.福建师范大学地理研究所,福州 350007;2.湿润亚热带山地生态国家重点实验室培育基地,福州 350007;  
3.福建省陆地灾害监测评估工程技术研究中心,福州 350007)

**摘要:**为探究极端降水的时空变化及其非平稳性特征,基于1972—2010年山美水库流域8个降水站点逐日降水数据,选取9个极端降水指数,利用Pre-Whitening Mann-Kendall(P-WM-K)方法分析流域极端降水的时空变化特征,并采用广义可加模型(generalized additive models for location, scale and shape, GAMLSS)检测极端降水的非平稳性特征。结果表明:在时间变化趋势上,极端降水频率指数中雨日数 $R_{10\text{ mm}}$ 和大雨日数 $R_{25\text{ mm}}$ 呈下降趋势,暴雨日数 $R_{50\text{ mm}}$ 呈上升趋势,且上升趋势达到0.05显著性水平;除降水总量 $P_{RCPTOT}$ 外,其余强度指数呈上升趋势,且均达到0.05显著性水平,其中极端降水量 $R_{95p}$ 线性倾向率达到30.5 mm/(10 a);在空间差异上, $R_{10\text{ mm}}$ 和极端降水强度指数在流域东南部呈现上升趋势,且上升趋势显著,西北部 $P_{RCPTOT}$ 下降较明显; $R_{10\text{ mm}}$ 和 $R_{25\text{ mm}}$ 呈平稳特征, $R_{50\text{ mm}}$ 全流域约50%的站点呈现非平稳特征,且以均值非平稳为主,除 $P_{RCPTOT}$ 外,其余强度指数均以非平稳特征为主,且主要表现为均值非平稳。未来山美水库流域极端降水量和不确定性增加,灾害风险增大。

**关键词:**极端降水;时空变化;非平稳性;GAMLSS模型;山美水库流域

中图分类号:TV125 文献标志码:A 开放科学(资源服务)标志码(OSID):



在全球气候变暖的背景下,全球及区域尺度极端降水事件的强度加大、频率增高,所带来的影响受到广泛关注<sup>[1-3]</sup>。许多研究<sup>[4-5]</sup>表明极端降水存在明显的区域差异。例如,从全球范围来看,自20世纪30年代起,美国极端降水事件的频率增加极其显著<sup>[6]</sup>,而加拿大极端降水事件的频率却无明显趋势<sup>[7]</sup>。欧洲年极端降水量表现为明显增加趋势<sup>[8-9]</sup>,而在西非和印度地区极端降水事件却呈现出下降趋势<sup>[10-11]</sup>。在中国,不同区域极端降水的变化趋势也存在显著的差异<sup>[12-13]</sup>。长江流域极端强降水总量呈显著增加趋势<sup>[14]</sup>,黄河流域极端降水频率呈显著增加趋势<sup>[15]</sup>,珠江流域极端降水强度略有上升<sup>[16]</sup>,淮河流域极端降水频率呈下降趋势<sup>[17]</sup>。因此不同区

域尺度、不同气候区的案例研究对丰富极端降水研究具有重要的意义。

在全球气候变化和人类活动的共同影响下,流域极端降水的概率分布往往发生变化,并可能呈现非平稳性特征<sup>[18]</sup>。目前,国外学者<sup>[19-20]</sup>主要基于不同的协变量探讨极端降水的非平稳特征。Vul等<sup>[21]</sup>将时间、最高温、平均温度和南方涛动周期等作为时变协变量,基于非平稳极值分布(the generalized extreme values, GEV)模型分析,发现美国极端降水的重现期显著缩短。Agilan等<sup>[22]</sup>基于6个协变量(时间、城市化、当地温度变化、全球气温年异常、El Niño-Southern Oscillation 和 Indian Ocean Dipole)分析印度极端降水的非平稳特征,并识别出

收稿日期:2021-07-07 修回日期:2021-11-18 网络出版时间:2021-11-23

网络出版地址:<https://kns.cnki.net/kcms/detail/13.1430.TV.20211123.1506.004.html>

基金项目:国家重点研发计划重点专项项目(2018YFE0206400);福建省科技厅省属公益类科研专项项目(2018R1034-3;2019R1002-3);福建省灾害天气重点实验室开放课题(2020KFKT01)

作者简介:宋铁燕(1997—),女,福建莆田人,主要从事水资源与环境研究。E-mail:sty\_yanzi@163.com

通信作者:陈莹(1982—),女,福建南平人,副教授,博士,主要从事水资源与环境研究。E-mail:chenying\_nju@163.com

研究区最佳协变量下的降水强度-持续时间-频率曲线。在国内,极端降水的非平稳特征作为新兴的研究课题,相关研究较少:吴孝情等<sup>[16]</sup>基于广义帕累托分布(generalized Pareto distribution, GPD)的参数时变特征提出时变(peak-over-threshold, POT)模型,研究发现时变 POT 模型可较好地刻画珠江流域降雨的非平稳性特征;黄婕等<sup>[23]</sup>利用经验模态分解法(empirical model decomposition, EMD)、Mann-Kendall 趋势检验法等发现了 1960—2012 年福建省前汛期、后汛期降水极值序列的非平稳特征明显加强;高洁<sup>[24]</sup>利用 Mann-Kendall 检验和广义可加模型(generalized additive models for location, scale and shape, GAMLS)研究雅砻江流域降水的非平稳特征,结果表明流域内降水极值的平稳性较好;韩丽等<sup>[25]</sup>以时间为协变量构建平稳和非平稳 GEV 模型探究了北京市最大月降水量的频率特征,发现最大月降水序列存在显著的非平稳特征。上述研究表明,在气候变化和人类活动的双重影响下,降水序列已呈现出非平稳的特征。但在研究对象上,多侧重于对年和月降水序列的非平稳特征进行分析,缺乏对极端降水特征变量的定量检测。

山美水库流域位于东南沿海经济发达的泉州市境内,该区受季风气候和台风影响显著,流域内城镇化发展迅速,人类活动影响剧烈,流域内极端降水的频次和强度均发生了变化<sup>[26-27]</sup>。本文以山美水库为研究对象,结合极端降水的频率和强度特征选取 9 个极端降水指数,采用 Pre-Whitening Mann-Ken-

dall(P-WM-K)分析 1972—2010 年研究区极端降水的趋势、均值序列和方差序列趋势检验,并基于 GAMLSS 探讨极端降水的非平稳特征,为研究区的防灾减灾提供科学依据。

## 1 研究区概况

山美水库位于福建省泉州市西北部的南安市境内( $25^{\circ}07'41''\text{N}$ ,  $118^{\circ}26'36''\text{E}$ ),是一座以灌溉为主兼具防洪和发电功能的大型水库,承担着下游地区 400 万人民群众生活生产用水和 4.33 万  $\text{hm}^2$  农田的灌溉用水任务,为保障泉州经济社会的可持续发展提供重要的水资源支撑<sup>[28-29]</sup>。山美水库流域集水面积为 1 023  $\text{km}^2$ ,多年平均径流量达 14 亿  $\text{m}^3$ 。研究区属于亚热带海洋性季风气候,多年平均气温约为 20  $^{\circ}\text{C}$ ,年降水量达到 1 600 mm 以上,多发生极端降水、洪涝等灾害。

## 2 数据来源与研究方法

### 2.1 数据来源

本文数据包括 1972—2010 年山美水库流域 8 个降水站点的日降水数据,数据来源于福建省水利厅,研究区概况见图 1。8 个降水站点的选择,基于各站点数据的长时序性、连续性,保证历史上没有站点迁站、相同时间序列内站点数量最多的原则进行筛选。所有降水数据均进行极值和时间一致性检验,并对异常值进行校验,以保证数据的完整性和准确性。

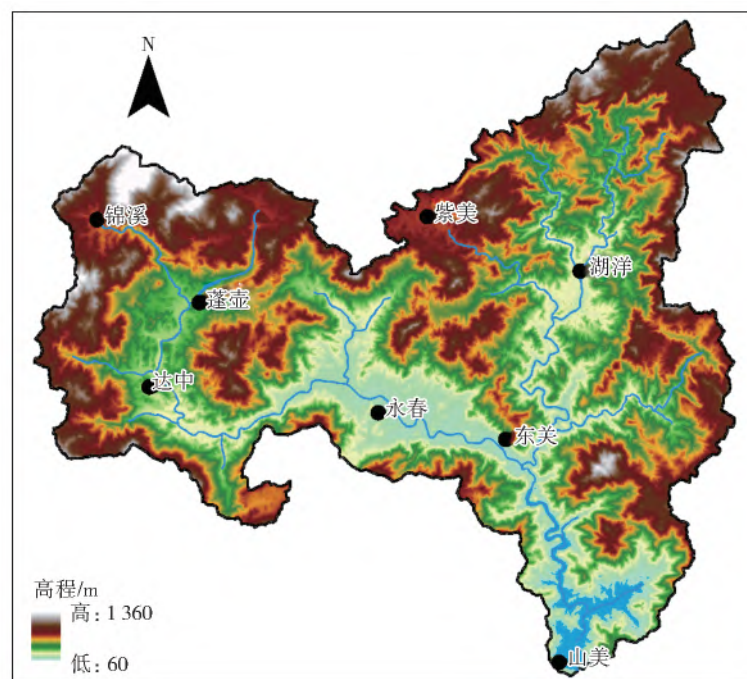


图 1 研究区概况  
Fig. 1 Location of the study area

## 2.2 研究方法

根据气候变化检测和指标专家组(expert team on climate change detection monitoring and indices, ETCCDMI)提供的极端降水指数,利用加拿大气象研究中心 Zhang 等<sup>[30]</sup>基于 R 语言开发的 RClimDex 软件进行极端降水指数的计算。选取其中代表降水频率和强度的 9 个指标(表 1)以表征极端降水特征,并基于中国降水量等级划分标准,将  $R_{n \text{ mm}}$  设定为  $R_{25 \text{ mm}}$  和  $R_{50 \text{ mm}}$  两个具体指标。因此,频率指数包括  $R_{10 \text{ mm}}$ 、 $R_{25 \text{ mm}}$  和  $R_{50 \text{ mm}}$  等,强度指数包括  $R_{X1\text{day}}$ 、 $R_{X5\text{day}}$ 、 $S_{DI}$ 、 $R_{95P}$  和  $P_{RCPTOT}$  等。

表 1 极端降水指数定义

Tab. 1 Definition of extreme precipitation indices

指数	名称	定义
$R_{10 \text{ mm}}$	中雨日数/d	每年降水量 $\geq 10 \text{ mm}$ 的日数
$R_{n \text{ mm}}$	自定义降水量日数/d	每年降水量 $\geq n \text{ mm}$ 的日数
$R_{95P}$	极端降水量/mm	每年日降水量 $>$ 第 95 百分位值的降水量之和
$R_{99P}$	极端强降水量/mm	每年日降水量 $>$ 第 99 百分位值的强降水量之和
$R_{X1\text{day}}$	极端日降水量/mm	每月最大 1 日降水量
$R_{X5\text{day}}$	极端 5 日降水量/mm	每月连续 5 天的最大降水量之和
$S_{DI}$	普通日降水强度/ $(\text{mm} \cdot \text{d}^{-1})$	每年降水量 $\geq 1.0 \text{ mm}$ 的总量与总日数之比
$P_{RCPTOT}$	降水总量/mm	每年日降水量大于 1 mm 的总量

### 2.2.1 P-WM-K 趋势检验

Mann-Kendall(M-K)检验法被广泛应用于水文和气象要素的趋势检验,但水文和气象要素的自相关性会影响 M-K 的检测能力<sup>[31-32]</sup>。与 M-K 检验相比,P-WM-K 检验可以消除样本自相关性对显著性放大的影响,从而更真实、合理地体现样本的趋势特征。此外,在与 M-K 检验<sup>[33-34]</sup>的总体趋势保持相一致的情况下,P-WM-K 检验能够得到更加客观的趋势。因此,采用可消除序列自相关的 P-WM-K 检验法进行趋势检验<sup>[35-36]</sup>。

### 2.2.2 广义可加模型(GAMLSS)

Rigby 等<sup>[37]</sup>提出的 GAMLSS 模型通过构建分布函数参数与多个解释变量间的线性与非线性、参数与非参数间的关系,进行径流量变化的模拟与归因分析。GAMLSS 模型具有灵活性,已被广泛应用于极端降水的模拟、径流变化的归因分析等<sup>[38-39]</sup>。Villarini 等<sup>[40-41]</sup>将 GAMLSS 模型运用到美国北卡罗莱纳州的洪峰流量变化特征检验和罗马地区的降水、气温序列的趋势分析中,均取得了较好的拟合效

果。基于分布函数位置、尺度和形状参数的 GAMLSS 模型在拟合位置、尺度和形状参数的基础上,通过拟合可加的半参数项或者非参数项、随机效应项,建立响应变量统计参数(位置、尺度、形状等)与解释变量的关系<sup>[37]</sup>,公式为

$$\mathbf{g}_k(\theta_k) = \mathbf{X}_k \boldsymbol{\beta}_k + \sum_{j=1}^m h_{jk}(x_{jk}) \quad (1)$$

式中: $\mathbf{g}_k(\cdot)$ 为  $k$  个统计参数的向量; $k$  表示具有  $k$  个参数(位置、尺度、形状参数), $k$  通常小于 4; $j$  为解释变量的个数, $j=1, \dots, m$ ; $\theta_k$  为长度为  $n$  的极端降水指数序列, $n$  代表年份时长; $\mathbf{X}_k$  是一个  $n \times m$  的解释变量矩阵; $\boldsymbol{\beta}_k$  是一个长度为  $m$  的参数向量; $h_{jk}(\cdot)$  代表分布参数和解释变量  $x_{jk}$  之间的函数关系,见表 2。

表 2 GAMLSS 模型常见分布函数类型

Tab. 2 Common distribution function types of GAMLSS

名称	简称	参数个数
Gamma	GA	2
Gumbel	GU	2
Log-Normal	LOGNO	2
Logistic	LO	2
Normal	NO	2
Inverse Gamma	IGAMMA	2
Inverse Gaussian	IG	2
Reverse Gumbel	RG	2
Weibull	WEI3	2

通过均值和方差序列的趋势变化来分析极端降水序列的非平稳性。不考虑随机项变量对函数的影响,以时间  $t$  作为唯一解释变量,从而得到极端降水指数序列均值  $\theta_1$  和方差  $\theta_2$  与解释变量时间  $t$  的关系(表 3)<sup>[35,42]</sup>为

$$\mathbf{g}_1(\theta_1) = t \boldsymbol{\beta}_1 \quad (2)$$

$$\mathbf{g}_2(\theta_2) = t \boldsymbol{\beta}_2 \quad (3)$$

## 3 结果与分析

### 3.1 极端降水指数的时空变化趋势

#### 3.1.1 时间变化趋势

基于泰森多边形法得到流域的面平均降水量,基于 5 年滑动平均线性以及 P-WM-K 趋势检验分析得到流域 1972—2010 年极端降水指数的时间变化趋势(图 2)和突变特征(图 3)。由图 2 可以看出:1972—2010 年山美水库流域  $R_{10 \text{ mm}}$  和  $R_{25 \text{ mm}}$  呈下降趋势; $R_{50 \text{ mm}}$  呈上升趋势,且线性倾向率为 0.4 d/(10 a)。在强度指数中,除  $P_{RCPTOT}$  外,其余极端降水强度指

标均呈现上升趋势。其中: $R_{95p}$  和  $R_{X5day}$  的上升趋势达到了 0.01 显著性水平, 线性倾向率分别为 40.0 mm/(10 a) 和 12.5 mm/(10 a);  $R_{99p}$ 、 $R_{X1day}$  和  $S_{DII}$  的上升趋势达到了 0.05 显著性水平, 线性倾向率分别为 24.2 mm/(10 a)、6.6 mm/(10 a) 和 0.4 mm/(10 a);  $P_{RCPTOT}$  呈现下降趋势, 且达到了

0.01 显著性水平。此外, 由图 3 可以看出, 极端降水指数在全流域均有发生突变, 且突变年份主要发生在 20 世纪 80 年代末和 90 年代初。山美水库流域除  $P_{RCPTOT}$  外, 其余强度指数呈现增加趋势, 表明该流域极端降水强度加大, 将面临更高的极端降水风险。

表 3 GAMLSS 模型常见趋势线型表达式

Tab. 3 Common trend line expressions of GAMLSS

编号	趋势线型	表达式	特征
1	$m$ 线性趋势, $\sigma$ 无趋势	$m=m_0+m_1t, \sigma=\sigma_0$	平稳
2	$m$ 无趋势, $\sigma$ 线性趋势	$m=m_0, \sigma=\sigma_0+\sigma_1t$	平稳
3	$m$ 抛物线型, $\sigma$ 无趋势	$m=m_0+m_1t+m_2t^2, \sigma=\sigma_0$	非平稳
4	$m$ 无趋势, $\sigma$ 抛物线型	$m=m_0, \sigma=\sigma_0+\sigma_1t+\sigma_2t^2$	非平稳
5	$m$ 线性趋势, $\sigma$ 线性趋势	$m=m_0+m_1t, \sigma=\sigma_0+\sigma_1t$	平稳
6	$m$ 抛物线型, $\sigma$ 线性趋势	$m=m_0+m_1t+m_2t^2, \sigma=\sigma_0+\sigma_1t$	非平稳
7	$m$ 线性趋势, $\sigma$ 抛物线型	$m=m_0+m_1t, \sigma=\sigma_0+\sigma_1t+\sigma_2t^2$	非平稳
8	$m$ 抛物线型, $\sigma$ 抛物线型	$m=m_0+m_1t+m_2t^2, \sigma=\sigma_0+\sigma_1t+\sigma_2t^2$	非平稳

注:  $m, \sigma$  分别为概率密度函数一、二阶矩, 即均值和方差。

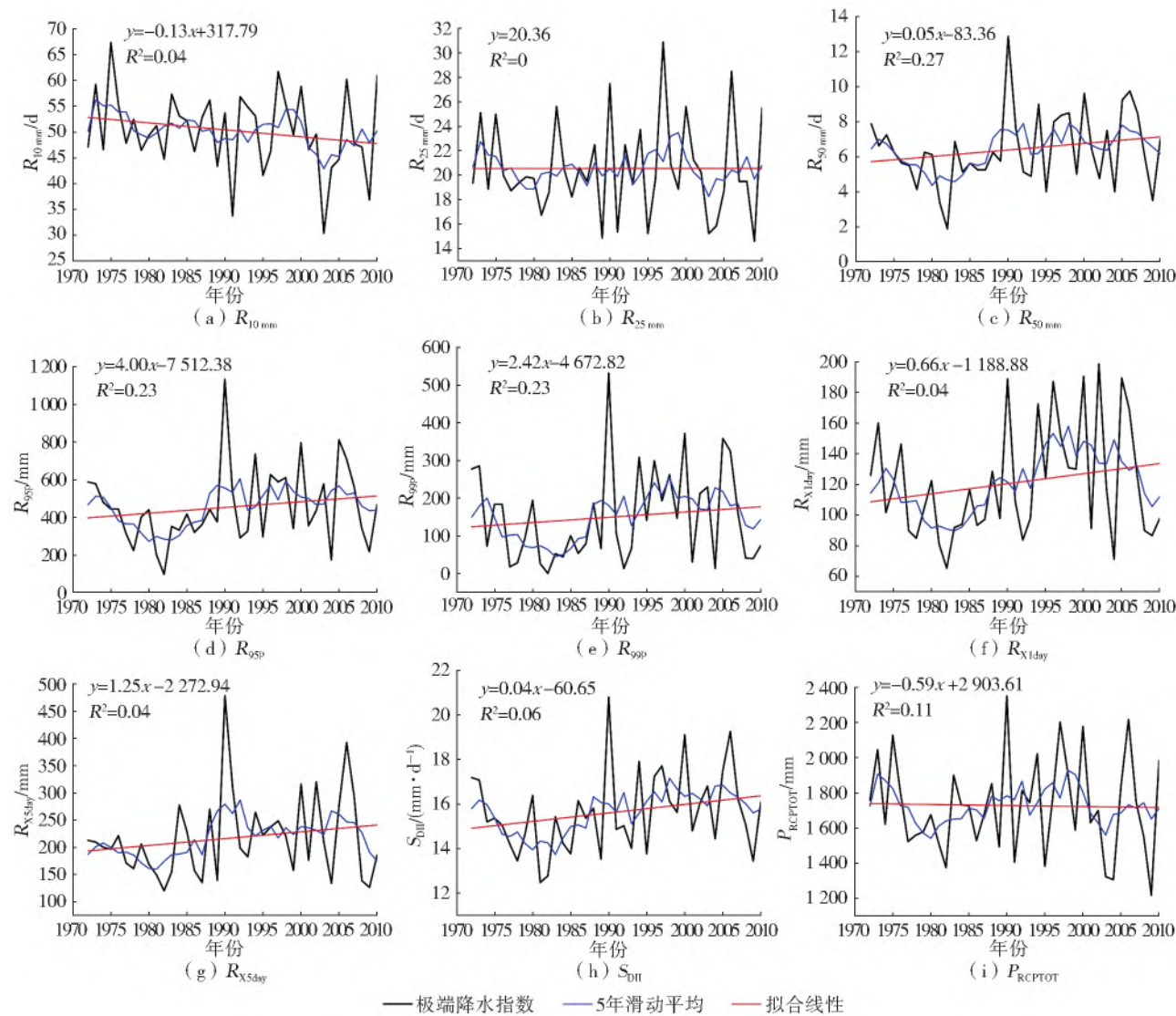


图 2 山美水库流域 1972—2010 年极端降水指数时间序列

Fig. 2 Time series of extreme precipitation index in Shanmei reservoir basin from 1972 to 2010

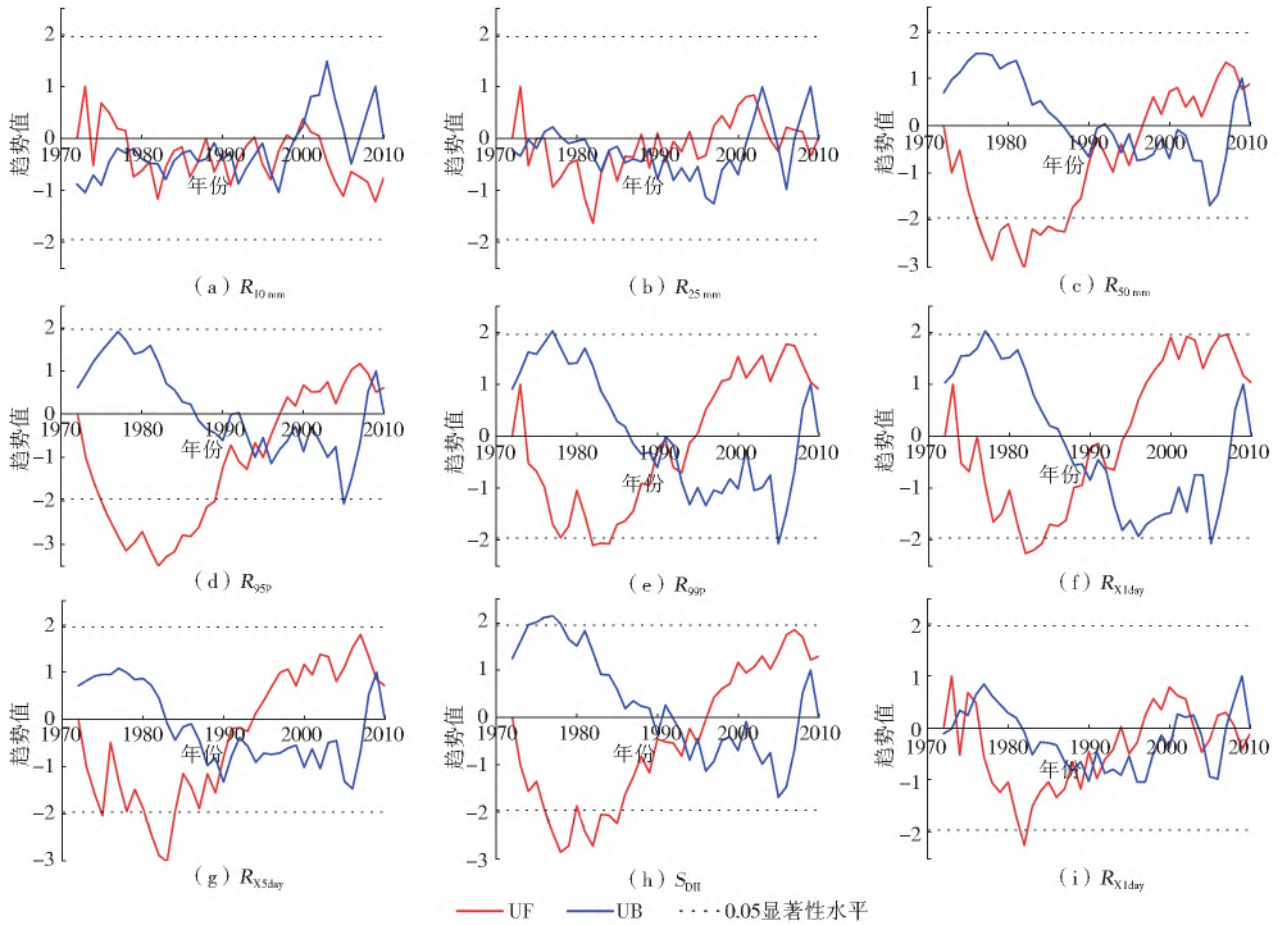


图3 基于P-WM-K方法1972—2010年山美水库流域极端降水指数的趋势检验

Fig. 3 Trend test of extreme precipitation index in Shammei reservoir basin from 1972 to 2010 based on P-WM-K method

### 3.1.2 空间差异性

基于山美水库流域8个站点极端降水指数的P-WM-K趋势检验结果,进行克里金插值得到全流域极端降水指数的变化趋势,见图4。就极端降水频率指数而言[图4(a)至4(c)]: $R_{10\text{mm}}$ 在全流域呈现下降趋势,且在达中站和蓬壶站均达到0.05显著性水平; $R_{25\text{mm}}$ 除南部(东关站和山美站)外,其余区域也表现为下降态势,但趋势不显著; $R_{50\text{mm}}$ 在流域西北部(锦溪站和蓬壶站)呈现很微弱的下降趋势,其余区域均呈现上升趋势,且在流域东南部(湖洋站、东关站和山美站)上升趋势达到0.05显著性水平。该结果表明,随着降雨量级的增加,极端降水频率指数在流域东南部呈现显著的增加趋势,即山美水库流域东南部暴雨的频次显著增加,流域面临的洪涝灾害风险将加大。

从流域极端降水强度指数的结果可以看出[图4(d)至4(i)]:流域东南部的极端降水强度指数主要呈现显著上升趋势,仅东关站和湖洋站的 $R_{99p}$ 、湖洋站和永春站的 $P_{RCPTOT}$ 的上升趋势不显著;西北部的锦溪站、蓬壶站和达中站的 $P_{RCPTOT}$ 下降较明显;北部的紫美站的 $R_{95p}$ 和 $S_{DII}$ 也有微弱的下降

趋势。

综上,1972—2010年山美水库流域东南部暴雨的频次显著增加,极端降水的强度显著增强,面临极端降水的风险性显著增加。

### 3.2 极端降水指数的非平稳特征

赤池信息量准则(Akaike information criterion, AIC)是一种用于评估统计模型拟合效果是否优良的标准<sup>[43]</sup>,AIC值越小表明模型拟合效果越好<sup>[35,44]</sup>。基于非平稳模型GAMLSS和残差分析原理,本文中Filliben<sup>[45]</sup>系数取0.981达到0.05显著性水平。考虑文章篇幅限制,本文仅展示 $R_{50\text{mm}}$ 、 $R_{X1\text{day}}$ 和 $S_{DII}$ 等极端降水指数的GAMLSS模型拟合参数及拟合残差,见表4。从 $R_{50\text{mm}}$ 来看,各站点拟合效果接近,AIC值范围为185~195,其中锦溪站拟合效果最好。相比于 $R_{50\text{mm}}$ , $R_{X1\text{day}}$ 拟合效果较差,AIC值范围为390~410,其中湖洋站拟合效果较好。相比于 $R_{50\text{mm}}$ 和 $R_{X1\text{day}}$ , $S_{DII}$ 拟合效果最好,AIC值在154~180,其中湖洋站和锦溪站拟合效果最好。其他指标的结果类似。总体上,模型在各站点的拟合效果较好,基本上都通过了0.05显著性检验。

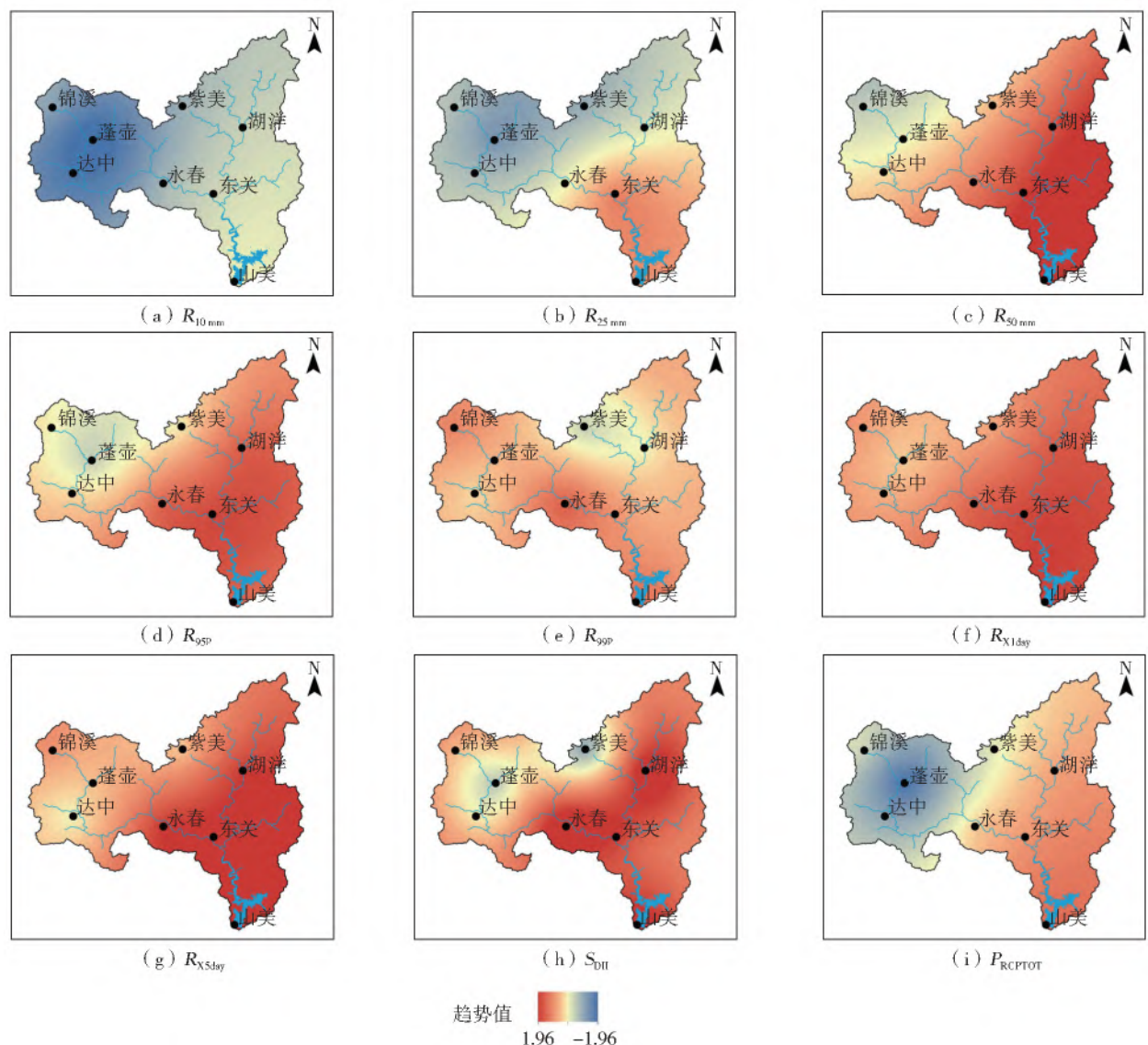


图 4 山美水库流域极端降水指数的 P-WM-K 趋势检验结果

Fig. 4 P-WM-K trend test of extreme precipitation indices in Shanmei reservoir basin

表 4 山美水库流域 GAMLSS 模型拟合参数及拟合残差

Tab. 4 Fitting parameters and residuals of GAMLSS model in the Shanmei reservoir basin

站点	AIC 值			均值			方差			Filliben 系数		
	$R_{50\text{mm}}$	$R_{X1\text{day}}$	$S_{\text{DII}}$									
达中	186.75	396.87	168.72	0	0	0.03	1.03	1.03	1.04	0.986*	0.985*	0.988*
东关	186.32	394.81	179.30	0	0	0	1.03	1.03	1.03	0.989*	0.983*	0.991*
湖洋	185.86	390.61	157.88	0	0.02	0	1.03	1.03	1.04	0.985*	0.988*	0.988*
锦溪	185.40	409.98	154.40	-0.01	0	0.01	1.08	1.03	1.06	0.990*	0.995*	0.990*
蓬壶	194.08	396.70	164.91	-0.01	0	-0.02	1.03	1.02	1.03	0.991*	0.994*	0.976
山美	193.45	390.11	179.95	0.01	0	0	0.97	1.03	1.03	0.977	0.994*	0.987*
永春	186.37	400.58	169.81	0	0.03	0	1.03	0.98	1.03	0.987*	0.991*	0.986*
紫美	195.24	399.29	166.65	0.01	0.01	0	1.05	1.03	1.03	0.995*	0.990*	0.986*

注: \* 代表达到 0.05 显著性水平。

基于 AIC 准则得到山美水库流域各站点极端降水指数的最优 GAMLSS 模型结果, 见表 5。从极端降水强度指数来看, WEI3 和 GA 则是出现次数最多的最优分布函数, 其中:  $R_{99\text{p}}$  在所有站点的最优分布函数为

次数最多的为 WEI3 和 GA。从极端降水强度指数来看, IGAMMA 和 RG 则是出现次数最多的最优分布函数, 其中:  $R_{99\text{p}}$  在所有站点的最优分布函数为

RG;  $R_{X5\text{day}}$ 除蓬壶站点外,在其余站点的最优分布函数为 IGAMMA。

表 5 各降水站点的非平稳特征

Tab. 5 Non-stationary characteristics of each precipitation station

站点	$R_{10\text{ mm}}$	$R_{25\text{ mm}}$	$R_{50\text{ mm}}$	$R_{95P}$	$R_{99P}$	$R_{X1\text{day}}$	$R_{X5\text{day}}$	$S_{DII}$	$P_{RCPTOT}$
达中	GA-1	NO-1	NO-8	WEI3-8	RG-3	IG-3	IGAMMA-2	LO-3	GA-2
东关	NO-2	GA-1	NO-3	WEI3-3	RG-3	IGAMMA-6	IGAMMA-3	GA-3	IG-3
湖洋	NO-2	RG-2	NO-3	RG-6	RG-8	IG-3	IGAMMA-8	RG-6	RG-2
锦溪	WEI3-4	GA-2	WEI3-2	RG-8	RG-1	IGAMMA-1	IGAMMA-2	RG-3	NO-2
蓬壶	LO-7	GA-5	WEI3-2	WEI3-2	RG-2	IG-2	IG-4	RG-2	NO-5
山美	LO-2	NO-2	WEI3-1	WEI3-1	RG-3	IGAMMA-3	IGAMMA-6	NO-3	LO-1
永春	WEI3-2	GA-2	GA-3	RG-6	RG-8	IGAMMA-2	IGAMMA-6	IGAMMA-6	GA-2
紫美	LO-2	IG-2	WEI3-2	RG-6	RG-8	IG-3	IGAMMA-8	IGAMMA-3	IG-2

注: 数字代表趋势线型, 趋势线型见表 3。

在变化环境下降水序列往往表现出非平稳性, 且非平稳性主要表现为均值序列的非平稳性和方差

序列的非平稳性。研究区各站点极端降水指数的非平稳特征结果见表 5 和图 5。

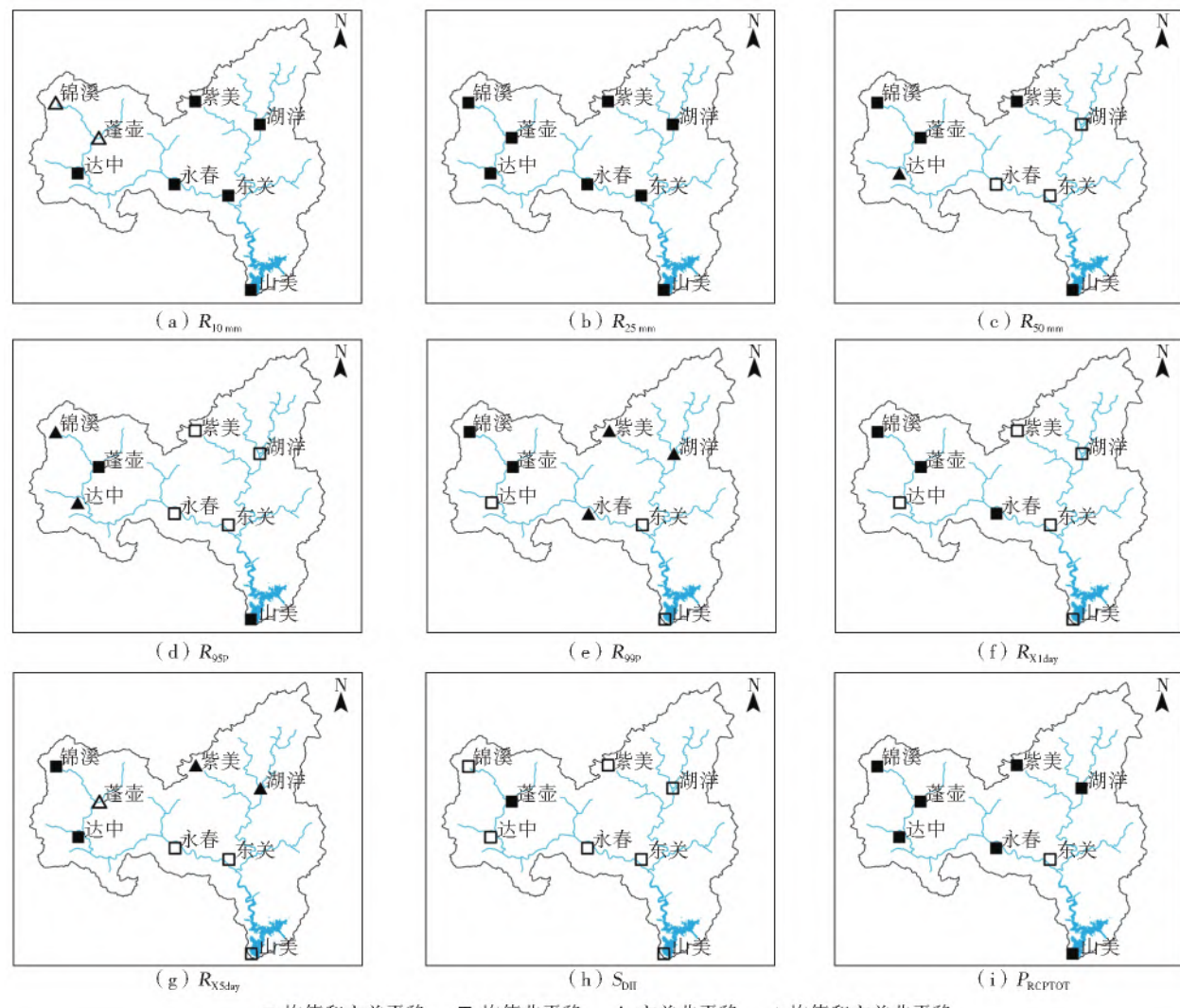


图 5 山美水库流域极端降水指数的非平稳性特征

Fig. 5 Non-stationary characteristics of extreme precipitation index in the Shanmei reservoir basin

从表 5、图 5 可以看出: 在频率指数中,  $R_{10\text{ mm}}$  和  $R_{25\text{ mm}}$  总体上呈现平稳特征, 仅  $R_{10\text{ mm}}$  在锦溪站和蓬壶站呈现方差非平稳, 而  $R_{50\text{ mm}}$  有 50% 的站点呈现

非平稳特征, 且以均值非平稳为主, 其中达中站呈现均值和方差均非平稳; 在强度指数中, 除  $P_{RCPTOT}$  外, 其余强度指数均以非平稳特征为主, 且主要表现为

均值非平稳;在站点的分布上,锦溪站和蓬壶站,除了  $R_{95P}$  和  $S_{DII}$  外,其余强度指数均呈现平稳性特征, $S_{DII}$  在全流域的站点(除蓬壶站)呈现均值非平稳。个别站点在某些指标中呈现均值和方差均非平稳,例如,紫美站和湖洋站在  $R_{99P}$  和  $R_{X5day}$  表现出均值和方差的非平稳。以上结果表明,随着降雨量级的增加,极端降水频率指数在山美水库流域逐渐呈现非平稳特征,即山美水库流域暴雨频次将呈现非平稳。降水频率和强度的非平稳将导致极端降水事件难以准确预估,增大了流域的洪涝灾害风险。

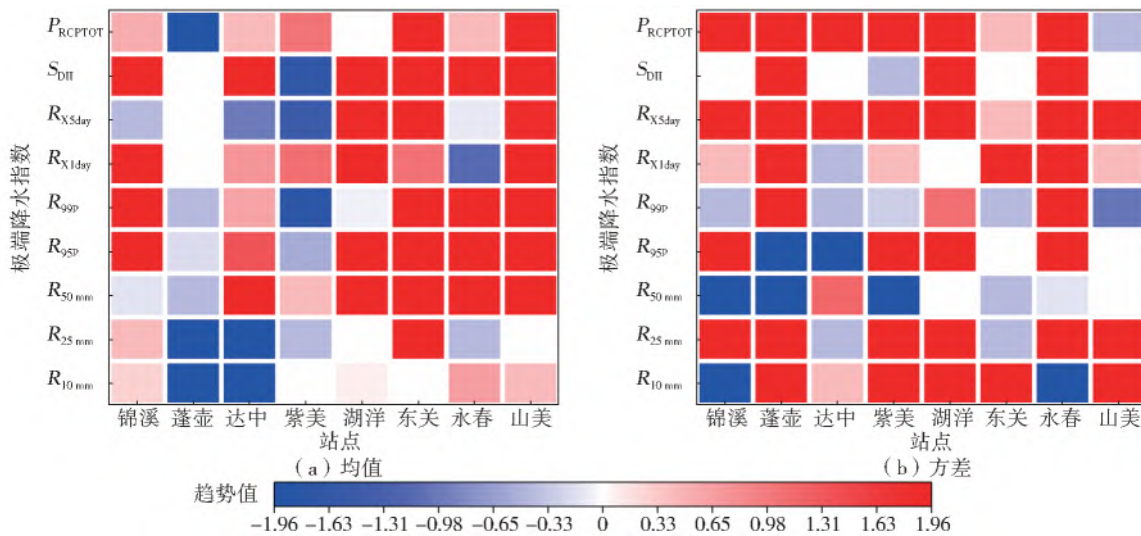


图 6 极端降水指数均值序列(a)和方差序列(b)的 P-WM-K 趋势检验结果

Fig. 6 P-WM-K trend test for mean and variance of extreme precipitation indices in the Shanmei reservoir basin

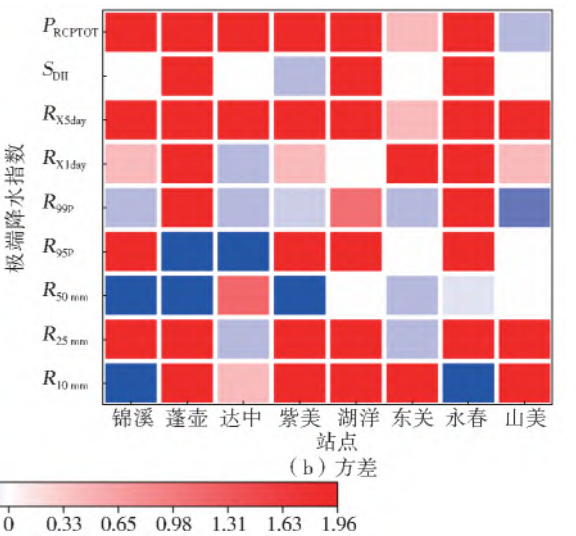
## 4 结 论

基于山美水库流域 8 个降水站点 1972—2010 年逐日降水数据,利用 P-WM-K 方法分析了流域极端降水变化的趋势特征,并采用 GAMLSS 模型探讨了极端降水的非平稳性,得到了以下结论:

山美水库流域中雨  $R_{10mm}$  和大雨  $R_{25mm}$  呈下降趋势,暴雨  $R_{50mm}$  呈上升趋势,且上升趋势达到 0.05 显著性水平;除  $P_{RCPTOT}$  外,其余强度指数均呈上升趋势,且达到 0.05 显著性水平,其中  $R_{95P}$  的增加趋势最显著,且线性倾向率达到 30.5 mm/(10 a)。此外,极端降水的频率和强度指标在 20 世纪 80 年代末和 90 年代初发生了突变。

流域极端降水指数的变化趋势在空间上具有差异性。 $R_{10mm}$  在全流域呈现下降趋势,且在达中站和紫美站均达到 0.05 显著性水平;北部站点  $R_{25mm}$  表现为下降态势,但趋势不显著; $R_{50mm}$  在流域东南部呈现上升趋势,且达到 0.05 显著性水平。流域东南部极端降水强度呈现显著上升趋势;西北部  $P_{RCPTOT}$  下降较明显。

基于 GAMLSS 模型得到的均值和方差进行 P-WM-K 趋势检验,检验结果见图 6。从图 6 可以看出:在均值序列中,流域东南部(湖洋站、东关站、永春站和山美站)极端降水指数基本呈现显著增加趋势,西北部极端降水频率指数主要呈现显著减少趋势;在方差序列中,极端降水强度指数主要表现为增加趋势,极端降水频率指数  $R_{50mm}$  在流域西北部主要表现为减少趋势。总体上,极端降水指数的均值和方差在流域东南部主要呈现增加趋势,西北部主要呈现减少趋势。



$R_{10mm}$  和  $R_{25mm}$  总体上呈现平稳特征,仅  $R_{10mm}$  在锦溪站和蓬壶站呈现方差非平稳; $R_{50mm}$  在全流域有 50% 的站点呈现非平稳特征,且以均值非平稳为主。除  $P_{RCPTOT}$ ,其余极端降水强度指数均以非平稳特征为主,且主要表现为均值非平稳。未来山美水库流域极端降水量和不确定性增加,灾害风险增大。

## 参 考 文 献(References):

- [1] IPCC. Climate Change 2014: Synthesis Report. Contribution of working groups I, II and III to the fifth assessment report of the intergovernmental panel on climate change [M]. Cambridge, UK: Cambridge University Press, 2014. DOI: 10.1017/epic.45156.001.
- [2] ALEXANDER L V, ZHANG X, PETERSON T C, et al. Global observed changes in daily climate extremes of temperature and precipitation[J]. Journal of Geophysical Research, 2006, 111(D5): 1042. DOI: 10.1029/2005JD006290.
- [3] COOLEY D. Return periods and return levels under climate change[M]. Springer Netherlands, 2013. DOI: 10.1007/978-94-017-8620-0\_3.

10. 1007/978-94-007-4479-0\_4.
- [4] CHEN Y R, CHU P S. Trends in precipitation extremes and return levels in the Hawaiian Islands under a changing climate[J]. International Journal of Climatology, 2015, 34 (15): 3913-3925. DOI: 10. 1002/joc. 3950.
- [5] ASADIEH B, KRAKAUER N Y. Global trends in extreme precipitation: climate models versus observations [J]. Hydrology and Earth System Sciences, 2015, 19 (2): 877-891. DOI: 10. 5194/hess-19-877-2015.
- [6] ZARAKARIZI M, RANA A, MORADKHANI H. Precipitation extremes and their relation to climatic indices in the Pacific northwest USA[J]. Climate Dynamics, 2018, 50 (11-12): 4519-4537. DOI: 10. 1007/s00382-017-3888-2.
- [7] KUNKEL K E. North American trends in extreme precipitation[J]. Natural Hazards, 2003, 29 (2): 291-305. DOI: 10. 1023/A:1023694115864.
- [8] VOGEL M M, ZSCHEISCHLER J, SENEVIRATNE S I. Varying soil moisture-atmosphere feedbacks explain divergent temperature extremes and precipitation projections in central Europe[J]. Earth System Dynamics, 2018, 9 (3): 1107-1125. DOI: 10. 5194/esd-9-1107-2018.
- [9] VOLOSCIUK C, MARAUN D, SEMENOV V A, et al. Rising Mediterranean Sea surface temperatures amplify extreme summer precipitation in central Europe[J]. Scientific Reports, 2016, 6: 32450. DOI: 10. 1038/srep32450.
- [10] AGUILAR E, BARRY A A, BRUNET M, et al. Changes in temperature and precipitation extremes in western central Africa, Guinea Conakry, and Zimbabwe, 1955-2006 [J]. Journal of Geophysical Research: Atmospheres, 2009, 114(D2). DOI: 10. 1029/2008JD011010.
- [11] VINCENT L, AGUILAR E, SAINDOU M, et al. Observed trends in indices of daily and extreme temperature and precipitation for the countries of the western Indian Ocean, 1961-2008 [J]. Journal of Geophysical Research Atmospheres, 2011, 116 (D10): 521-541. DOI: 10. 1029/2010JD015303.
- [12] 田庆云. 气候变化条件下非平稳极端降水频率特征研究[D]. 北京: 中国地质大学(北京), 2020. (TIAN Q Y. Research on the frequency characteristics of non-stationary extreme precipitation under climate change [D]. Beijing: China University of Geosciences (Beijing), 2020. (in Chinese))
- [13] 程诗悦, 秦伟, 郭乾坤, 等. 近 50 年我国极端降水时空变化特征综述[J]. 中国水土保持科学, 2019, 17(3): 155-161. (CHENG S Y, QIN W, GUO Q K, et al. Summary of the characteristics of temporal and spatial changes of extreme precipitation in China in the past 50 years[J]. Science of Soil and Water Conservation, 2019, 17(3): 155-161. (in Chinese)) DOI: 10. 16843/j.sswc. 2019. 03. 020.
- [14] 苏布达, 姜彤, 任国玉, 等. 长江流域 1960—2004 年极端强降水时空变化趋势[J]. 气候变化研究进展, 2006, 3 (1): 9-14. (SU B D, JIANG T, REN G Y, et al. The temporal and spatial trends of extreme heavy rainfall in the Yangtze River basin from 1960 to 2004[J]. Climate Change Research Progress, 2006, 3 (1): 9-14. (in Chinese)) DOI: CNKI: SUN: QHBH. 0. 2006-01-002.
- [15] 靳莉君, 王春青, 王鹏, 等. 黄河流域极端降水特征分析[J]. 水资源与水工程学报, 2016, 27 (6): 44-48. (JIN L J, WANG C Q, WANG P, et al. Analysis on the characteristics of extreme precipitation in the Yellow River basin[J]. Journal of Water Resources and Water Engineering, 2016, 27 (6): 44-48. (in Chinese))
- [16] 吴孝情, 陈晓宏, 唐亦汉, 等. 珠江流域非平稳性降雨极值时空变化特征及其成因[J]. 水利学报, 2015, 46 (9): 1055-1063. (WU X Q, CHEN X H, TANG Y H, et al. Characteristics and causes of temporal and spatial variation of non-stationary rainfall extremes in the Pearl River basin[J]. Journal of Hydraulic Engineering, 2015, 46 (9): 1055-1063. (in Chinese)) DOI: 10. 13243/j.cnki. slxb. 20141415.
- [17] 潘欣, 尹义星, 王小军. 1960—2014 年淮河流域极端降水发生时间的时空特征[J]. 高原气象, 2019, 38 (2): 377-385. (PAN X, YIN Y X, WANG X J. Spatio-temporal characteristics of the occurrence timing of extreme precipitation in the Huai River basin from 1960 to 2014 [J]. Plateau Meteorology, 2019, 38(2): 377-385. (in Chinese))
- [18] MILLY P C D, BETANCOURT J, FALKENMARK M, et al. Climate change-Stationarity is dead: Whither water management[J]. Science, 2008, 319 (5863): 573-574. DOI: 10. 1126/science. 1151915.
- [19] SERAGO J M, VOGEL R M. Parsimonious nonstationary flood frequency analysis[J]. Advances in Water Resources, 2018, 112: 1-16. DOI: 10. 1016/j.advwatres. 2017. 11. 026.
- [20] THIOMBIANO A N, ST-HILAIRE A, ADLOUNI S E, et al. Nonlinear response of precipitation to climate indices using a non-stationary Poisson-generalized Pareto model: Case study of southeastern Canada[J]. International Journal of Climatology, 2018, 38: 875-888. DOI: 10. 1002/joc. 5415.

- [21] VUL T M, MISHRA A. Nonstationary frequency analysis of the recent extreme precipitation events in the United States [J]. *Journal of Hydrology*, 2019, 575 (2019): 999-1010. DOI: 10.1016/j.jhydrol.2019.05.090.
- [22] AGILAN V, UMAMAHESH N V. What are the best covariates for developing non-stationary rainfall intensity-duration-frequency relationship [J]. *Advances in Water Resources*, 2017, 101: 11-22. DOI: 10.1016/j.advwatres.2016.12.016.
- [23] 黄婕,高路,陈兴伟,等.降水极值的非平稳性特征及其重现期研究:以福建省为例[J].北京师范大学学报(自然科学版),2016,52(5):603-609. (HUANG J, GAO L, CHEN X W. et al. Study on the non-stationary characteristics and return period of precipitation extreme value: Taking Fujian Province as an example [J]. *Journal of Beijing Normal University (Natural Science Edition)*, 2016, 52(5): 603-609. (in Chinese)) DOI: 10.16360/j.cnki.jbnuns.2016.05.012.
- [24] 高洁.基于GAMLSS的雅鲁江流域极端降水时空特性研究[J].*水力发电*,2019,45(1):13-17,56. (GAO J. Study on the temporal and spatial characteristics of extreme precipitation in the Yalong River basin based on GAMLSS[J]. *Hydropower*, 2019, 45 (1): 13-17, 56. (in Chinese)) DOI: CNKI: SUN: SLFD. 0. 2019-01-005.
- [25] 韩丽,黄俊雄,周娜,等.非平稳条件下北京市最大月降水量频率特征分析[J].*水文*,2021,41(2):32-37,108. (HAN L, HUANG J X, ZHOU N, et al. Frequency characteristics analysis of the maximum monthly precipitation in Beijing under non-stationary conditions[J]. *Hydrology*, 2021, 41(2): 32-37,108. (in Chinese)) DOI: 10.19797/j.cnki.1000-0852.20190410.
- [26] 吴杰峰,陈兴伟,高路,等.人类活动对晋江流域径流演变影响的分析与定量评估[J].*南水北调与水利科技*,2017,15(2):65-72,79. (WU J F, CHEN X W, GAO L, et al. Analysis and quantitative assessment of the impact of human activities on the evolution of runoff in the Jinjiang River basin [J]. *South-to-North Water Transfers and Water Science & Technology*, 2017, 15(2): 65-72,79. (in Chinese)) DOI: 10.13476/j.cnki.nsbdqk.2017.02.010.
- [27] 林木生,陈兴伟,陈莹.晋江西溪流域土地利用覆被变化及其洪水响应分析[J].*南水北调与水利科技*,2011,9(1):80-83. (LIN M S, CHEN X W, CHEN Y. Land use cover change and flood response analysis in the Xixi basin of Jinjiang River [J]. *South-to-North Water Transfers and Water Science & Technology*, 2011, 9(1): 80-83. (in Chinese)) DOI: CNKI: SUN: NSBD. 0. 2011-01-022.
- [28] 王迪,刘梅冰,陈兴伟,等.基于CMIP5和SWAT的山美水库流域未来蓝绿水时空变化特征[J].*南水北调与水利科技(中英文)*,2021,19(3):446-458. (WANG D, LIU M B, CHEN X W, et al. Future blue-green water temporal and spatial characteristics of Shanmei reservoir basin based on CMIP5 and SWAT [J]. *South-to-North Water Transfers and Water Science & Technology*, 2021, 19 (3): 446-458. (in Chinese)) DOI: 10.13476/j.cnki.nsbdqk.2021.0048.
- [29] 吴丽娜,陈莹,陈兴伟,等.气候变化下山美水库流域未来径流量变化[J].*亚热带资源与环境学报*,2019,14(4):18-22,35. (WU L N, CHEN Y, CHEN X W, et al. Future runoff changes in Shanmei reservoir basin under climate change [J]. *Journal of Subtropical Resources and Environment*, 2019, 14 (4): 18-22,35. (in Chinese)) DOI: 10.19687/j.cnki.1673-7105.2019.04.003.
- [30] ZHANG X B, YANG F. RClimate(1.0) user manual [R]. Climate Research Branch Environment Canada Downsview, Ontario Canada, 2004.
- [31] 章诞武,丛振涛,倪广恒.基于中国气象资料的趋势检验方法对比分析[J].*水科学进展*,2013,24(4):490-496. (ZHANG D W, CONG Z T, NI G H. Comparative analysis of trend test methods based on Chinese meteorological data[J]. *Advances in Water Science*, 2013, 24(4): 490-496. (in Chinese)) DOI: 10.14042/j.cnki.32.1309.2013.04.019.
- [32] 王跃峰.闽江流域降水径流时序变化特征与洪旱事件识别[D].福州:福建师范大学,2014. (WANG Y F. Temporal variation characteristics of precipitation and runoff in Minjiang River basin and identification of flood and drought events[D]. Fuzhou: Fujian Normal University, 2014. (in Chinese))
- [33] MANN H B. Nonparametric test against trend[J]. *Econometrica*, 1945, 13 (3): 245-259. DOI: 10.2307/1907187.
- [34] KENDALL M, GIBBONS J D. Rank correlation method[M]. Oxford, UK: Oxford University Press, 1990.
- [35] 雷享勇,高路,马苗苗,等.鄱阳湖流域极端降水时空分布和非平稳性特征[J].*应用生态学报*,2021,32(9):3277-3287. (LEI X Y, GAO L, MA M M, et al. Temporal and spatial distribution and non-stationary characteristics of extreme precipitation in Poyang Lake basin [J]. *Journal of Applied Ecology*, 2021, 32 (9): 3277-3287. (in Chinese)) DOI: 10.13287/j.1001-9332.202109.017.
- [36] YUE S, WANG C Y. Applicability of prewhitening to

- eliminate the influence of serial correlation on the Mann-Kendall test [J]. Water Resources Research, 2002, 38: 41-47. DOI: 10.1029/2001WR000861.
- [37] RIGBY R A, STASINOPoulos D M. Generalized additive models for location, scale and shape[J]. Journal of the Royal Statistical Society: Series C (Applied Statistics), 2005, 54 (3): 507-554. DOI: 10.1111/j.1467-9876.2005.00510.x.
- [38] GAO L, HUANG J, CHEN X, et al. Risk of extreme precipitation under nonstationarity conditions during the second flood season in the southeastern coastal region of China [J]. Journal of Hydrometeorology, 2016, 18 (3): 669-681. DOI: 10.1175/JHM-D-16-0119.1.
- [39] GAO L, HUANG J, CHEN X, et al. Contributions of natural climate changes and human activities to the trend of extreme precipitation [J]. Atmospheric Research, 2018, 205: 60-69. DOI: 10.1016/j.atmosres.2018.02.006.
- [40] VILLARINI G, SMITH J A, NAPOLITANO F. Non-stationary modeling of a long record of rainfall and temperature over Rome [J]. Advances in Water Resources, 2010, 33 (10): 1256-1267. DOI: 10.1016/j.advwatres.2010.03.013.
- [41] VILLARINI G, SMITH J A, SERINALDI F, et al. Flood frequency analysis for nonstationary annual peak records in an urban drainage basin [J]. Advances in Water Resources, 2009, 32(8): 1255-1266. DOI: 10.1016/j.advwatres.2009.05.003.
- [42] 孙鹏,孙玉燕,张强,等.淮河流域洪水极值非平稳性特征[J].湖泊科学,2018,30(4):1123-1137. (SUN P, SUN Y Y, ZHANG Q, et al. Non-stationary characteristics of extreme flood values in the Huaihe River basin[J]. Lake Science, 2018, 30 (4): 1123-1137. (in Chinese)) DOI:CNKI:SUN:FLKX.0.2018-04-025.
- [43] AKAIKE H. A new look at the statistical model identification[J]. IEEE Transactions on Automatic Control, 1974, 19(6): 716-723. DOI: 10.1007/978-1-4612-1694-0\_16.
- [44] 高斌,肖伟华,鲁帆,等.基于GAMLSS模型的三峡库区主汛期降雨非一致性分析[J].水土保持研究,2021,28(5):152-158,171. (GAO B, XIAO W H, LU F, et al. Analysis of rainfall inconsistency in the main flood season in the Three Gorges reservoir area based on GAMLSS model[J]. Research on Soil and Water Conservation, 2021, 28 (5): 152-158, 171. (in Chinese)) DOI: 10.13869/j.cnki.rswc.2021.05.018.
- [45] LI X H, HU Q. Spatiotemporal changes in extreme precipitation and its dependence on topography over the Poyang Lake basin, China [J]. Advances in Meteorology, 2019, 22: 1-15. DOI: 10.1155/2019/1253932.

## Temporal and spatial variation and non-stationary characteristics of extreme precipitation in the Shanmei reservoir basin

SONG Tieyan<sup>1</sup>, CHEN Ying<sup>1,2,3</sup>, LEI Xiangyong<sup>1</sup>, CHEN Xingwei<sup>1,2,3</sup>, GAO Lu<sup>1,2,3</sup>, LIU Meibing<sup>1,2,3</sup>, DENG Haijun<sup>1,2,3</sup>

(1. Institute of Geography, Fujian Normal University, Fuzhou 350007, China; 2. Cultivation Base of State Key Laboratory of Subtropical Mountain Ecology, Fuzhou 350007, China; 3. Fujian Provincial Engineering Research Center for Monitoring and Assessing Terrestrial Disasters, Fuzhou 350007, China)

**Abstract:** The probability distribution of extreme precipitation in the Shanmei reservoir basin is expected to change due to the dual influence of global climate change and human activities, showing non-stationary characteristics. Therefore, investigating the temporal and spatial trend characteristics and the non-stationarity of the extreme precipitation are valuable for policy decisions.

Based on the daily precipitation data of 8 meteorological stations in the Shanmei reservoir basin from 1972 to 2010, 9 extreme precipitation indices including 6 intensity indices and 3 frequency indices were used to describe the extreme precipitation characteristics. The Pre-Whitening Mann-Kendall (P-WM-K) method was adopted to analyze the temporal and spatial trend changes of extreme precipitation, and the generalized additive models for location, scale, and shape (GAMLSS) was employed to characterize the non-stationarities in the 9 indices in the Shanmei reservoir basin.

The number of moderate precipitation days ( $R_{10\text{mm}}$ ) and the number of heavy rain days ( $R_{25\text{mm}}$ ) showed a downward trend while the number of very heavy rain days ( $R_{50\text{mm}}$ ) showed an upward trend with a 0.05 significant level. Except for the total precipitation ( $P_{RCPTOT}$ ), the other intensity indices (daily intensity ( $S_{DII}$ ), very wet day precipitation ( $R_{95P}$ ), extremely wet day precipitation ( $R_{99P}$ ), max 1-day precipitation ( $R_{X1day}$ ) and the max 5-day precipitation ( $R_{X5day}$ )) increased significantly. The linear trend rate of  $R_{95P}$  reached 30.5 mm/(10 a). The extreme precipitation indices had abrupt changes in the whole basin, and the mutation years mainly occurred in the late 1980s and early 1990s. In terms of spatial variation,  $R_{10\text{mm}}$  and  $R_{25\text{mm}}$  showed a download

(下转第 364 页)

Taking Langfang urban water system as an example, the water system connectivity evaluation system of the plain city river network was constructed to quantitatively evaluate the water system connectivity status of eight water system connectivity schemes. The results showed that there were differences in the three criterion levels of water system pattern, structural connectivity, and hydraulic connectivity for different working conditions. Combining the comprehensive evaluation scores and the grade cut-off values, the optimal water system connectivity solution can be obtained to improve the water system connectivity of the whole river network for Langfang city and could suggest that the river network should open the Shengli branch canal, Shengfeng branch canal, and Xiaoliuzhuang branch canal in the water transmission process, and dredge and desilt of the three branch canals with serious pollution according to the local actual situation.

The system can evaluate the water system connectivity of the plain city river network in a more comprehensive way, and reflect the water system connectivity status of different water system connectivity schemes. The hydraulic connectivity index can reflect the mobility of water bodies in water systems. The calculation method of the hydraulic connectivity index in the hydraulic connectivity criterion layer was improved, so that it can be applied to the whole river network, making up for the limitation that the index was only applicable to the calculation of a single river in the past. To address the limitations, the evaluation of water system connectivity by index values can not take into account the influence of multiple factors, based on the water system connectivity evaluation system. The AHP-entropy integrated evaluation method was used to evaluate different water system connectivity schemes in terms of water system pattern, structural connectivity, and hydraulic connectivity to obtain the final evaluation scores of different water system connectivity schemes, to determine the optimal solution for water system connectivity and to make reasonable planning suggestions for the whole river network. The overall connectivity of the river network is optimal after connecting the three heavily polluted rivers with other rivers.

**Key words:** water system connectivity; evaluation system; hydraulic connectivity; comprehensive evaluation; plain urban river network

(上接第 337 页)

trend for all the stations, and reaches a 0.05 significant level in Dazhong and Zimei Stations.  $R_{25\text{ mm}}$  showed a downward trend for the stations in the exception of the Dongguan and Shanmei Stations while the trend was not significant. The  $R_{50\text{ mm}}$  and extreme precipitation intensity indices showed an upward trend in the southeastern part of the basin (Yongchun Station, Huyang Station, Dongguan Station, and Shanmei Station), and the trend was significant. The  $P_{\text{RCPTOT}}$  had decreased significantly in the northwest of the basin. The GAMLSS model was fitted well to each precipitation station, and the Filliben coefficient passed the 0.05 significance level.  $R_{10\text{ mm}}$  and  $R_{25\text{ mm}}$  showed stationary characteristics. The  $R_{50\text{ mm}}$  showed non-stationary characteristics at 50% of the stations in the basin, and that was dominated by mean non-stationary. Except for  $P_{\text{RCPTOT}}$ , the other intensity indices mainly showed non-stationary characteristics which mainly manifested as the mean non-stationary. Under the non-stationary conditions, the mean and variance of the extreme precipitation indices was mainly characterized by an increasing trend in the southeastern basin, and mainly showed a decreasing trend in the northwest.

In light of climate variability and anthropogenic activities, the stable environment of extreme precipitation events in the Shanmei reservoir basin had been disturbed. The intensity of extreme precipitation and  $R_{50\text{ mm}}$  increased significantly in the Shanmei reservoir basin, especially in the southeastern part of the basin. This showed non-stationary characteristics in the study area. The intensity of extreme precipitations as well as uncertainty would increase, which may lead to more related disasters in the future.

**Key words:** extreme precipitation; temporal and spatial variation; non-stationarity; GAMLSS model; Shanmei reservoir basin